J. Fac. Pharm. Ankara / Ankara Ecz. Fak. Derg., 48(3): 975-992, 2024
Doi: 10.33483/jfpau.1417289

ORIGINAL ARTICLE / ÖZGÜN MAKALE

IN SILICO TRIAL APPROACHES BETWEEN PHYTOCHEMICAL COMPOSITION OF *VERBENA OFFICINALIS AND* LIVER CANCER TARGETS

VERBENA OFFICINALIS'İN FİTOKİMYASAL BİLEŞİMİ İLE KARACİĞER KANSERİ HEDEFLERİ ARASINDAKİ İN SİLİKO DENEME YAKLAŞIMLARI

Hatice AKKAYA[1]*, Aydın OZMALDAR[2]

[1]Health Sciences University, Faculty of Pharmacy, Department of Biochemistry, 34668, Istanbul, Türkiye
[2]Krosgen Biotechnology, Department of IT, 34750, Istanbul, Türkiye

ABSTRACT

Objective: *The abundance of bioactive metabolites in Verbena officinalis explains the biological benefits and folkloric use of the plant. Liver cancer is an extremely heterogeneous malignant disease compared to other defined tumors. To explore the potential therapeutic value of bioactive metabolites in Verbena officinalis, this study aimed to filter secondary metabolites, conduct ADME-Tox assessments, perform drug similarity tests, and analyze with molecular dynamic simulations. The objective was to evaluate how potential drug candidates derived from Verbena officinalis behave in biological systems and assess their potential toxicity risks.*
Material and Method: *Ligands selected from the ADME assay were utilized in in silico molecular docking studies against Glucose-6-phosphate dehydrogenase enzyme in the oxidative part of the pentose phosphate pathway, which is crucial for liver diseases. These studies were conducted using Autodock Vina embedded in Chimera 1.16. Molecular dynamics simulations were performed with the AMBER16.*
Result and Discussion: *When the ADME test results were evaluated, 88 secondary metabolites were identified as ligands. Among all the ligands evaluated against Glucose-6-phosphate dehydrogenase enzyme, which is the key enzyme of the pentose phosphate pathway, quercetin flavonoid was determined to be the most active ligand with a docking score of -8.1 kcal/mol and binding energy of -118.51 kcal/mol. A molecular dynamics simulation performed for 300 nanoseconds confirmed that quercetin can remain stable in its microenvironment. The activity of this metabolite is worthy of further testing in vitro and in vivo as it may highlight a therapeutic modality within the pentose phosphate pathway.*
Keywords: *In silico, liver cancer, pentose phosphate pathway, toxicitiy, Verbena officinalis*

ÖZ

Amaç: *Verbena officinalis bitkisinde bulunan biyoaktif metabolitlerin bolluğu, bitkinin biyolojik faydalarını ve halk arasındaki kullanımını açıklar. Karaciğer kanseri, diğer tanımlanmış tümörlere kıyasla son derece heterojen kötü huylu bir hastalıktır. Verbena officinalis'teki biyoaktif metabolitlerin potansiyel terapötik değerini keşfetmek için, bu çalışma ikincil metabolitleri filtrelemeyi, ADME-Tox değerlendirmeleri yapmayı, ilaç benzerlik testleri gerçekleştirmeyi ve moleküler dinamik simülasyonları ile analiz etmeyi amaçlamıştır. Hedef, Verbena officinalis'ten elde edilen potansiyel ilaç adaylarının biyolojik sistemlerde nasıl davrandığını değerlendirmek,*

* **Corresponding Author / Sorumlu Yazar:** Hatice Akkaya
e-mail / e-posta: hatice.akkaya@sbu.edu.tr, **Phone / Tel.:** +902167778777

Submitted / Gönderilme : 09.01.2024
Accepted / Kabul : 11.07.2024
Published / Yayınlanma : 10.09.2024

potansiyel toksisite risklerini değerlendirmekti.
Gereç ve Yöntem: *ADME testinden seçilen ligandlar, karaciğer hastalıkları için önemli olan pentoz fosfat yolunun oksidatif kısmındaki Glukoz-6-fosfat dehidrogenaz enzimi için in siliko moleküler bağlanma çalışmalarında kullanıldı. Bu çalışmalar Chimera 1.16'ya gömülü Autodock Vina kullanılarak gerçekleştirildi. Moleküler dinamik simülasyonları AMBER16 programı ile gerçekleştirildi.*
Sonuç ve Tartışma: *ADME test sonuçları değerlendirildiğinde, 88 sekonder metabolit ligand olarak belirlendi. Pentoz fosfat yolunun anahtar enzimi olan Glukoz-6-fosfat dehidrogenaz enzimine karşı değerlendirilen tüm ligandlar arasında, kuersetin flavonoidi, -8.1 kcal/mol bağlanma skoru ve -118.51 kcal/mol bağlanma enerjisi ile en etkin ligand olarak belirlendi. 300 nanosaniye boyunca yapılan moleküler dinamik simülasyonu ise quercetinin bulunduğu mikroçevrede stabil olarak kalabildiğini doğruladı. Bu metabolitin aktivitesi, pentoz fosfat yolu içinde terapötik bir modaliteyi ortaya koyabileceği için in vitro ve in vivo testlerle daha ileri incelenmeye değerdir.*
Anahtar Kelimeler: *İn siliko, karaciğer kanseri, pentoz fosfat yolu, toksisite, Verbena officinalis*

INTRODUCTION

Computer-aided drug discovery (CADD) plays a pivotal role in identifying and optimizing hit compounds, thus advancing them through the drug discovery pipeline [1]. Its interdisciplinary essence, incorporating chemoinformatics, bioinformatics, molecular modeling, and data mining, has notably contributed to the endeavors of drug discovery. The integration of artificial intelligence, especially machine learning and deep learning, has propelled CADD's progress in recent years [2]. Despite encountering challenges and occasional disillusionments stemming from misuse and inflated expectations, CADD remains an indispensable tool in modern drug discovery initiatives [3].

Moreover, in the realm of drug discovery, *Verbena officinalis (V. officinalis)* is the main species in the genus *Verbena* of the *Verbenaceae* family [4]. This family has more than a thousand species, consisting of trees, shrubs, as well as herbaceous plants [5]. A monograph on "*Vervain herb*" was published in the European Pharmacopoeia (6th Edition) in 2008 regarding this plant, which is known as a traditional medicinal raw material. The main groups of secondary metabolites of *V. officinalis* herb, which has a rich chemical composition, consist of iridoids, phenylpropanoid glycosides, flavonoids, phenolic acids, terpenoids, carbohydrates, sterols, fatty acids and essential oils [6]. Therapeutic practices using *V. officinalis* plant extracts, which are used in traditional medicine as well as traditional Chinese medicine, are supported by scientific evidence [7,8]. It is known that *V. officinalis* plant helps in the treatment of urinary tract disorders, has supportive properties in the treatment of menstrual disorders [9,10], nervous system disorders [11] malaria and rheumatism.

In addition to being an antimicrobial and secretolytic raw material, it has also been stated to be an anti-inflammatory and antibacterial agent in skin diseases [10]. It has been stated that *V. officinalis* inhibits the mechanism or execution of neuronal apoptosis [12], increases serotonin, norepinephrine and dopamine levels in nerve terminals [13], its essential oil stimulates apoptosis through caspase-3 activation [14], and its flavonoids and polyphenols have been reported to have a gastroprotective effect [15]. In addition, it has various biological and pharmacological activities such as analgesic [16], antioxidant [17], hepatoprotective [18], antinephrosis [19], antiprostatitis [20]. In another study, it was stated that the anticonvulsant effect of *V. officinalis* flavonoids and phenolic acid residues probably occurs through activation of the GABAA receptor [11]. Pentose phosphate pathway (PPP), which is the important pathway for ribonucleotide synthesis, is the most important source of NADPH (reduced form of Nicotinamide Adenine Dinucleotide Phosphate), which is of great importance for cellular functions such as fatty acid synthesis and scavenging of reactive oxygen species [21]. The pentose phosphate pathway (PPP), in which cancer cells extensively use glucose, branches from glycolysis and is crucial for cancer cell metabolism. In the oxidative phase of PPP, glucose is converted into glucose 6-phosphate (G6P), which is then oxidized to 6-phosphogluconolactone by the rate-limiting enzyme glucose 6-phosphate dehydrogenase (G6PD), producing NADPH. Another source of NADPH in PPP is the conversion of 6-phosphogluconate into ribose (ribulose) 5-phosphate by 6-phosphogluconate dehydrogenase (6PGD) [22]. Glucose-6-phosphate dehydrogenase (G6PD) plays a crucial role in liver cancer, especially hepatocellular carcinoma. Its high expression in hepatocellular carcinoma affects

energy metabolism and redox balance through the PPP, leading to changes in NADPH levels and increased oxidative stress, promoting cancer progression. Abnormal activation of G6PD enhances cell proliferation and survival in hepatocellular carcinoma, making it a potential diagnostic marker closely associated with patient prognosis [23,24]. Additionally, G6PD is important in other cancers like glioma, breast cancer, and multiple myeloma, affecting energy metabolism and redox homeostasis [25]. Elevated G6PD levels in these cancers stimulate cell proliferation by increasing NADPH production and reducing reactive oxygen species (ROS). Targeting G6PD and the PPP could be a promising therapeutic approach by disrupting cancer cell growth and survival through modulation of cellular redox balance.

By leveraging "*in silico*" methods such as molecular docking, ADME-Tox studies, and drug similarity analyses [26-29], this study aims to evaluate the potential of *V. officinalis* metabolites as drug candidates targeting liver cancer. Through the integration of CADD principles with pharmacological research on *V. officinalis*, this study represents a multidisciplinary effort to explore novel avenues in drug discovery and therapeutic interventions.

MATERIAL AND METHOD

Selection of Receptors and Ligands

Through a review of the literature [6,30], metabolites from *V. officinalis* were collected, and SMILES notations were extracted from the PubChem database (https://pubchem.ncbi.nlm.nih.gov). The energy of the molecules was minimized using the Build Structure tool integrated into Chimera, and the resulting ligands were saved in Mol2 format for docking studies. The target protein G6PD (PDBID: 6E08) was retrieved from the RCSB Protein Data Bank (https://www.rcsb.org/) [31,32]. After removing small molecules and water molecules from the 3D crystallographic protein structure, polar hydrogen atoms and charges were added, and the final protein structure was saved as a Mol2 file.

Computer-Based Analysis of Pharmacokinetics and Toxicity Tests

Drug similarity as well as oral bioavailability (Lipinski's rule of 5) [33] of the compounds selected as drug candidates were evaluated with SwissADME (http://www.swissadme.ch/), which is used especially to estimate pharmacokinetic properties. Ligands that comply with this rule have been studied in molecular docking. The ProTox-II server (http://tox.charite.de/protoc_II;) was used to provide an estimate of the primary toxicity properties and acute toxicity values of the secondary metabolite of *V. officinalis* that was most active based on docking results and to help establish its safety profile for oral administration [29].

Molecular Docking

The ligand molecule was prepared in PDBQT format and utilized with the AutoDock Vina command prompt [25]. The active site of the ligand bound to G6PD was determined by averaging the coordinates of the x, y, and z axes. A grid box search area measuring 25 × 25 × 25 Å was defined [32,34]. Following this, the ligands were positioned within the enzyme's active site and the resulting binding energy (score) between the ligands and targets was computed.

Molecular Dynamic Simulation

The molecular dynamics simulation of the G6PD-quercetin complex was performed with the AMBER16 package using the ff14SB force field for the protein [35], with a 2-femtosecond time step in a truncated octahedron box containing 20530 explicit TIP3P water molecules [36]. The molecular dynamics simulations were performed for a total of 300 nanoseconds (ns). The Antechamber program, part of AmberTools, was used to parameterize quercetin, and to assign partial charges, RESP fitting approach was used. Heavy atom-hydrogen bond distances were fixed with SHAKE algorithm, and the Langevin thermostat was employed to maintain the system's temperature at 310 K. To account for electrostatic interactions, the Particle Mesh Ewald method was used. Additionally, three sodium ions (Na^+) were introduced to neutralize the system's overall charge.

Software Used

Windows 10 Microsoft operating system was installed. SwissADME online tool was used for drug design and evaluation. Protox II was used to help establish a safety profile via oral routes [29]. The UCSF Chimera (1.16) program (https://www.cgl.ucsf.edu/chimera/download.html) was run for docking with AutoDock Vina [28]. Protein and chemical (ligand) structures were searched in Protein Data Bank (https://www.rcsb.org/) and PubChem, respectively. IGemDOCK V2.1 was used to calculate the binding energies of the ligands. For the interaction poses of the resulting complex structure, Plip-tool (https://plip-tool.biotec.tu-dresden.de/plip-web/plip/index) [37] and ProteinsPlus web servers (https://proteins.plus/) were used. The AMBER16 program [38] was used for the molecular dynamics (MD) simulations, which were run on supercomputers at the TÜBİTAK ULAKBİM High Performance and Grid Computing Center (TRUBA).

RESULT AND DISCUSSION

In this study, the molecular interactions of phytochemicals contained in *V. officinalis*, whose anticoccidial [41] and antioxidant potentials [42] were reported in *in silico* studies, with G6PD in cancer treatment were evaluated. It is thought that quercetin, one of the phytochemicals evaluated according to its pharmacokinetics, pharmacodynamics, drug similarity, physiochemical properties, low binding affinity value and toxicological analysis, is physiologically active and can be considered as an oral drug. Cancer cells need to divide and grow rapidly, which requires the production of high amounts of NADPH. It can be said that reducing the effect of the pentose phosphate pathway by inhibiting G6PD activity is theoretically a strategy in the treatment of liver cancer and other types of cancer [27,43].

ADME is an approach to study the ADME properties of drugs using computer-based models and calculations, which plays an important role in drug development processes [44]. Lipinski's Rule of Five Drug Molecules is a set of guidelines stating that a drug candidate must possess four specific physical and chemical properties within acceptable limits for its oral bioavailability to be high [33]. The suitability of 109 compounds belonging to *V. officinalis* as drug candidates was obtained using the SwissADME server. According to the results, it was determined that the log P value of all 109 compounds was less than 5, and the molecular weight of 96 compounds was within the acceptable range (MW<500). The number of H-bond acceptors (≤10) and donors (≤5) falls within the acceptable range for 90 and 86 compounds, respectively. 83 compounds were identified in the topological polar surface area range (TPSA; <140). The number of rotatable bonds is within the acceptable range (≤10) for 100 compounds (Table 1). Considering these results, molecular docking studies were applied to investigate the anticancer activity in the next step. For liver cancer, 87 Verbane-based compounds (iridoids, flavonoids, phenolic acids, terpenoids, carbohydrates, sterols, fatty acids, essential oils) were used as ligands, and G6PD was used as the receptor (Table 2). While the binding energy of quercetin was 118.51 kcal/mol, its docking score was determined as -8.1 kcal/mol. According to all the tested ligands, it can be said that the structure that binds most effectively to G6PD is quercetin. In this way, the physicochemical properties of the most active structure quercetin determined were examined in more detail (Table 2). When the complex structure of quercetin and G6PD is examined, hydrophobic interactions with the amino acid tyrosine (Y480), hydrogen bonds with the amino acids arginine (Arg366) and aspartate (Asp394), and π-stacking structures with the amino acids tyrosine (Tyr374) and tryptophan (Trp482) are observed (Figure 1a,b).

In biological systems, molecular recognition is based on the principle of recognizing specific attractive interactions between two molecules [45]. These interactions may help quercetin and the G6PD complex fold correctly and enable the desired chemical reactions to occur. Additionally, understanding how interactions can be controlled at the molecular level may be important for potential drug design or biotechnological applications (Table 1, Figure 2). When looking at the interactions of the original crystal structure of G6PD with the nicotinamide adenine dinucleotide phosphate (NADP) ligand [46], it was observed that it formed H bonds and pi interactions with the same amino acids, but hydrophobic interactions were not observed. This indicates that the binding conditions of molecular interactions or molecular conformations have changed. Such changes can sometimes be associated with the emergence of a binding site where one molecule recognizes or binds to another, sometimes facilitating the binding

of a ligand to the active site of the protein or providing specificity in molecular recognition processes. In a related study [47], it was observed that in the different three-dimensional structure (2BH9) of the G6PD enzyme, quercetin forms four hydrogen bonds with Gly (38), Asp (42), Arg (72), and Arg (246) amino acids. These diverse binding interactions may impact ligand binding, conformation, and interaction mechanisms, leading to varied biological effects, inhibitor activities, or therapeutic properties. Consequently, the formation of distinct amino acid bonds between the same ligand and enzymes with different three-dimensional structures can result in diverse biological and pharmacological outcomes.

Table 1. List of pharmacokinetic properties of 109 metabolites of *Verbane officinalis*

	Compound	Physicochemical properties						Lipo-philicity	Water Solubility	Pharmaco-kinetics	Drug-likeness
		Molecular weight (gr/mol)	Number of rotatable bonds	Number of H-bond acceptors	Number of H-bond donors	Molar Refractivity	TPSA (Å²)	Log Po/w	LogS (ESOL)	GI absorbtion	Lipinski/violation
1	verbenalin	388.37	5	10	4	86.4	151.98	2.19	-0.97	Low	Yes; 0 violation
2	hastatoside	210.23	2	4	0	52.86	52.60	2.10	-1.40	High	Yes; 0 violation
3	7-hydroxy-dehydro-hastatoside	418.35	5	12	6	88.70	192.44	1.37	-0.63	Low	No; 2 violations: NorO>10, NHorOH>5
4	aucubin	346.33	4	9	**6**	77.15	149.07	1.44	0.18	Low	Yes; 1 violation: NHorOH>5
5	verbeofflin	240.21	5	5	1	57.42	57.42	1.71	-1.54	High	Yes; 0 violation
6	verbascoside	624.59	11	15	9	148.12	245.29	3.00	-2.87	Low	No; 3 violations: MW>500, NorO>10, NHorOH>5
7	2,4-diacetyl-O-verbascoside	708.66	15	17	7	167.90	257.43	3.06	-3.82	Low	No; 3 violations: MW>500, NorO>10, NHorOH>5
8	sover-bascoside	624.6	11	15	9	148.42	245.29	2.33	-4.18	Low	No; 3 violations: MW>500, NorO>10, NHorOH>5
9	4-acetyl-O-soverbas-coside	666.6	13	16	8	158.16	251.36	3.16	-3.35	Low	No; 3 violations: MW>500, NorO>10, NHorOH>5
10	3,4-diacetyl-O-soverbas-coside	708.66	15	17	7	167.9	257.43	3.00	-5.62	Low	No; 3 violations: MW>500, NorO>10, NHorOH>5
11	eukovoside	666.6	13	16	8	157.9	251.36	2.27	-4.61	Low	No; 3 violations: MW>500, NorO>10, NHorOH>5
12	campenoside II	490.5	8	10	4	120.82	151.98	3.26	-3.03	Low	Yes; 0 violation
13	betonyoside A	654.6	12	16	9	154.05	254.52	3.20	-2.49	Low	No; 3 violations: MW>500, NorO>10, NHorOH>5
14	cistanoside D	652.6	13	15	7	157.36	223.29	2.59	-3.32	Low	No; 3 violations: MW>500, NorO>10, NHorOH>5
15	Leucoscep-toside	638.6	12	15	8	152.89	234.29	2.78	-3.09	Low	No; 3 violations: MW>500, NorO>10, NHorOH>5
16	5,7,4'-Tri-hydroxy-8-nethoxy-flavone	300.26	2	6	3	80.48	100.13	2.25	-3.99	High	Yes; 0 violation
17	diosmetin	300.26	2	6	3	80.48	100.13	2.47	-4.06	High	Yes; 0 violation
18	artemetin	388.4	6	8	1	102.40	96.59	3.59	-4.44	High	Yes; 0 violation
19	quercetin	302.23	1	7	5	78.03	131.36	1.63	-3.16	High	Yes; 0 violation
20	kaempferol	286.24	1	6	4	76.01	111.13	1.7	-3.31	High	Yes; 0 violation
21	Luteolin	286.24	1	6	4	76.01	111.13	1.86	-3.71	High	Yes; 0 violation
22	luteolin 7-O-diglucuronide	638.5	7	18	10	141.33	303.57	1.16	-3.23	Low	No; 3 violations: MW>500, NorO>10, NHorOH>5

Table 1 (*continue*). List of pharmacokinetic properties of 109 metabolites of *Verbane officinalis*

	Compound	Physicochemical properties						Lipo-phillicity	Water Solubility	Pharmaco-kinetics	Drug-likeness
		Molecular weight (gr/mol)	Number of rotatable bonds	Number of H-bond acceptors	Number of H-bond donors	Molar Refractivity	TPSA (Å²)	Log Po/w	LogS (ESOL)	GI absorbtion	Lipinski/violation
23	luteolin 7-O-glucuronide	462.4	4	12	7	108.74	207.35	1.55	-3.41	Low	No; 2 violations: NorO>10, NHorOH>5
24	luteolin 7-O-glucoside	448.4	4	11	7	108.13	190.28	1.83	-3.65	Low	No; 2 violations: NorO>10, NHorOH>5
25	6-hydroxy-luteolin glycoside	464.4	4	12	8	110.16	210.51	1.67	-3.51	Low	No; 2 violations: NorO>10, NHorOH>5
26	luteolin-7-O-rutinoside	610.5	7	16	10	140.52	269.43	2.81	-3.0	Low	No; 3 violations: MW>500, NorO>10, NHorOH>5
27	apigenin	270.24	1	5	3	73.99	90.90	1.89	-3.94	High	Yes; 0 violation
28	apigenin 7-O-diglucuronide	622.5	7	17	9	139.71	283.34	2.03	-3.36	Low	No; 3 violations: MW>500, NorO>10, NHorOH>5
29	apigenin 7-O-glucoside	432.18	4	10	6	106.11	170.05	2.17	-3.78	Low	Yes; 1 violation: NHorOH>5
30	isoramnetin	316.26	2	7	4	82.50	120.36	2	-3.89	High	Yes; 0 violation
31	pedalitin	316.26	2	7	4	82.50	120.36	1.25	-3.76	High	Yes; 0 violation
32	scutellarein	286.24	1	6	4	76.01	111.13	2.08	-3.79	High	Yes; 0 violation
33	scutellarein 7-O-glucuronide	462.4	4	12	7	108.74	207.35	1.11	-3.27	Low	No; 2 violations: NorO>10, NHorOH>5
34	scutellarein 7-O-glucoside	448.4	4	11	7	108.13	190.28	1.75	-3.05	Low	No; 2 violations: NorO>10, NHorOH>5
35	chlorogenic acid	354.31	5	9	6	83.50	164.75	0.96	-1.62	Low	Yes; 1 violation: NHorOH>5
36	ferulic acid	194.18	3	4	2	51.63	66.76	1.62	-2.11	High	Yes; 0 violation
37	protocatechuic acid	154.12	1	4	3	37.45	77.76	0.66	-1.86	High	Yes; 0 violation
38	4,5-O-dicaffeoyl-quinic acid	516.4	9	12	7	126.9	211.28	1.25	-3.65	Low	No; 3 violations: MW>500, NorO>10, NHorOH>5
39	1,5-dicaffeoyl-quinic acid	516.4	9	12	7	126.9	211.28	1.11	-3.65	Low	No; 3 violations: MW>500, NorO>10, NHorOH>5
40	rosmarinic acid	360.3	7	8	5	91.40	144.52	1.17	-3.44	Low	Yes; 0 violation
41	carnosol	330.4	1	4	2	92.83	66.76	2.97	-4.77	High	Yes; 0 violation
42	carnosolic acid	348.4	2	5	4	96.59	97.99	2.33	-4.31	High	Yes; 0 violation
43	rosmanol	346.4	1	5	3	93.99	86.99	2.50	-4.25	High	Yes; 0 violation
44	isorosmanol	346.4	1	5	3	93.99	86.99	2.59	-4.25	High	Yes; 0 violation
45	ursolic acid	456.7	1	3	2	136.91	57.53	3.71	-7.23	Low	Yes; 1 violation: MLOGP>4.15
46	3-epiursolic acid	456.7	1	3	2	136.91	57.53	3.71	-7.23	Low	Yes; 1 violation: MLOGP>4.15
47	arabinose	150.13	0	5	4	29.77	90.15	-0.39	1.13	Low	Yes; 0 violation
48	galactose	180.16	1	6	5	35.74	110.38	0.24	1.15	Low	Yes; 0 violation
49	galacturonic acid	194.14	1	7	5	36.35	127.45	-0.19	0.50	Low	Yes; 0 violation
50	glucose	180.16	1	6	5	35.74	110.38	0.24	1.15	Low	Yes; 0 violation
51	mannose	180.16	1	6	5	35.74	110.38	0.24	1.15	Low	Yes; 0 violation
52	rhamnose	164.16	0	5	4	34.57	90.15	0.66	0.46	High	Yes; 0 violation
53	Xylose	150.13	0	5	4	29.77	90.15	-0.39	1.13	Low	Yes; 0 violation
54	stigmasterol	370.61	4	1	1	118.33	20.23	4.53	-6.67	Low	Yes; 1 violation: MLOGP>4.15
55	daucosterol	576.85	9	6	4	165.61	99.38	4.98	-7.70	Low	Yes; 1 violation: MW>500

Table 1 (*continue*). List of pharmacokinetic properties of 109 metabolites of *Verbane officinalis*

	Compound	Physicochemical properties						Lipo-phillicity	Water Solubility	Pharmaco-kinetics	Drug-likeness
		Molecular weight (gr/mol)	Number of rotatable bonds	Number of H-bond acceptors	Number of H-bond donors	Molar Refractivity	TPSA (Å²)	Log Po/w	LogS (ESOL)	GI absorbtion	Lipinski/violation
56	β-sitosterol	414.71	6	1	1	133.23	20.23	4.79	-7.90	Low	Yes; 1 violation: MLOGP>4.15
57	cornudentanone	378.5	15	5	0	107.58	69.67	4.08	-4.99	High	Yes; 0 violation
58	oleic acid	282.5	15	2	1	89.94	37.30	4.27	-5.41	High	Yes; 1 violation: MLOGP>4.15
59	3-epioleanolic acid	456.7	1	3	2	136.65	57.53	3.89	-7.32	Low	Yes; 1 violation: MLOGP>4.15
60	isobornyl formate	182.26	2	2	0	51.92	26.30	2.43	-3.55	High	Yes; 0 violation
61	citral (geranial)	152.23	4	1	0	49.44	17.07	2.47	-2.43	High	Yes; 0 violation
62	limonene	136.23	1	0	0	47.12	0.00	2.72	-3.50	Low	Yes; 0 violation
63	carvone	150.22	1	1	0	47.32	17.07	2.27	-2.41	High	Yes; 0 violation
64	1.8-cineole	154.25	0	1	0	47.12	9.23	2.58	-2.52	High	Yes; 0 violation
65	hepten-3-one	112.17	4	1	0	35.49	17.07	2.03	-1.47	High	Yes; 0 violation
66	α-terpineol	154.25	1	1	1	48.80	20.23	2.51	-2.87	High	Yes; 0 violation
67	anethole	148.20	2	1	0	47.83	9.23	2.55	-3.11	High	Yes; 0 violation
68	β-pinene	136.23	0	0	0	45.22	0.00	2.59	-3.31	Low	Yes; 1 violation: MLOGP>4.15
69	thymol	150.22	1	1	1	48.01	20.23	2.32	-3.19	High	Yes; 0 violation
70	methyl heptenone	126.20	3	1	0	40.30	17.07	2.23	-1.61	High	Yes; 0 violation
71	carvacrol	150.22	1	1	1	48.01	20.23	2.24	-3.31	High	Yes; 0 violation
72	trans-carveol	152.23	1	1	1	48.28	20.23	2.50	-2.68	High	Yes; 0 violation
73	isopiperitone	152.23	1	1	1	47.80	17.07	2.38	-2.51	High	Yes; 0 violation
74	α-pinene	136.23	0	0	0	45.22	0.00	2.63	-3.51	Low	Yes; 1 violation: MLOGP>4.15
75	piperitone	152.23	1	1	0	47.80	17.07	2.38	-2.51	High	Yes; 0 violation
76	cis-carveol	152.23	1	1	1	48.28	20.23	2.50	-2.68	High	Yes; 0 violation
77	terpinen-4-ol	154.25	1	1	1	48.80	20.23	2.51	2.78	High	Yes; 0 violation
78	β-phellandrene	136.23	1	0	0	47.12	0.00	2.65	-2.79	Low	Yes; 0 violation
79	geraniol	154.25	4	1	1	50.40	20.23	2.75	-2.78	High	Yes; 0 violation
80	β-terpineol	154.25	1	1	1	48.80	20.23	2.41	-2.32	High	Yes; 0 violation
81	sabinene	136.23	1	0	0	45.22	0.00	2.65	-2.57	Low	Yes; 1 violation: MLOGP>4.15
82	cinerone	150.22	2	1	0	47.32	17.07	2.39	-1.75	High	Yes; 0 violation
83	p-cymene	134.22	1	0	0	45.99	0.00	2.51	-3.63	Low	Yes; 1 violation: MLOGP>4.15
84	nerol	154.25	4	1	1	50.40	20.23	2.75	-2.78	High	Yes; 0 violation
85	linalol	154.25	4	1	1	50.44	20.23	2.70	-2.40	High	Yes; 0 violation
86	(E)-β-ocimene	136.23	3	0	0	48.76	0.00	2.80	-3.17	Low	Yes; 0 violation
87	borneol	154.25	0	1	1	46.60	20.23	2.29	-2.51	High	Yes; 0 violation
88	iso-pinocamphone	152.23	0	1	0	45.90	17.07	2.18	-2.21	High	Yes; 0 violation
89	o-cymene	134.22	1	0	0	45.99	0.00	2.43	-3.81	Low	Yes; 1 violation: MLOGP>4.15
90	γ-terpinene	136.23	1	0	0	47.12	0.00	2.73	-3.45	Low	Yes; 0 violation
91	caryophyllene oxide	220.35	0	1	1	68.27	12.53	3.15	-3.45	High	Yes; 0 violation
92	spathulenol	220.35	0	1	1	68.34	20.23	2.88	-3.17	High	Yes; 0 violation

Table 1 (*continue*). List of pharmacokinetic properties of 109 metabolites of *Verbane officinalis*

	Compound	Physicochemical properties						Lipo-phillicity	Water Solubility	Pharmaco-kinetics	Drug-likeness
		Molecular weight (gr/mol)	Number of rotatable bonds	Number of H-bond acceptors	Number of H-bond donors	Molar Refractivity	TPSA (Å²)	Log Po/w	LogS (ESOL)	GI absorbtion	Lipinski/violation
93	α-curcumane	202.33	4	0	0	69.55	0.00	3.50	-4.52	Low	Yes; 1 violation: MLOGP>4.15
94	β-caryophyllene	204.35	0	0	0	68.78	0.00	3.29	-3.87	Low	Yes; 1 violation: MLOGP>4.15
95	trans-nerolidol	222.37	7	1	1	74.00	20.23	3.64	-3.80	High	Yes; 0 violation
96	bicyclosesquiphellandrene	204.35	1	0	0	69.04	0.00	3.33	-4.00	Low	Yes; 1 violation: MLOGP>4.15
97	δ-cadinene	204.35	1	0	0	69.04	0.00	3.32	-3.43	Low	Yes; 1 violation: MLOGP>4.15
98	germacene D	204.35	1	0	0	70.68	0.00	3.32	-4.03	Low	Yes; 1 violation: MLOGP>4.15
99	α-muurolene	204.35	1	0	0	69.04	0.00	3.38	-3.61	Low	Yes; 1 violation: MLOGP>4.15
100	bicyclogermacrene	204.35	0	0	0	68.78	0.00	3.34	-3.72	Low	Yes; 1 violation: MLOGP>4.15
101	cis-muurola-4(14).5-diene	204.35	1	0	0	69.04	0.00	3.33	-4.00	Low	Yes; 1 violation: MLOGP>4.15
102	isocaryophylene oxide	220.35	0	1	1	68.27	12.53	3.15	-3.45	High	Yes; 0 violation
103	β-cedrene	204.35	0	0	0	66.88	0.00	3.18	-4.16	Low	Yes; 1 violation: MLOGP>4.15
104	α-copaene	204.35	1	0	0	67.14	0.00	3.40	-3.86	Low	Yes; 1 violation: MLOGP>4.15
105	β-elemene	204.35	3	0	0	70.42	0.00	3.37	-4.76	Low	Yes; 1 violation: MLOGP>4.15
106	β-cubenene	204.35	1	0	0	67.14	0.00	3.39	-4.01	Low	Yes; 1 violation: MLOGP>4.15
107	α-humulene	204.35	0	0	0	70.42	0.00	3.27	-3.97	Low	Yes; 1 violation: MLOGP>4.15
108	α-7-epi-selinene	204.35	1	0	0	68.78	0.00	3.31	-4.32	Low	Yes; 1 violation: MLOGP>4.15
109	isoledene	204.35	0	0	0	67.14	0.00	3.26	-3.67	Low	Yes; 1 violation: MLOGP>4.15

Table 2. Binding energies and affinities of 88 ligands selected from *Verbena officinalis* to the G6PDH protein structure

Group of metabolites	Compounds	Pubchem CID	Binding energy (kcal/mol)	Binding affinity (kcal/mol)
Iridoids				
	hastatoside	92043450	-105.7	-6.8
	verbeofflin	101875571	-99.33	-5.9
Flavonoids				
	5,7,4'-Trihydroxy-8-methoxyflavone	5322078	-109.45	-7.3
	diosmetin	5281612	-109.88	-8.1
	artemetin	5320351	-109.18	-7.0
	quercetin	5280343	-115.06	-8.1
	kaempferol	5280863	-105.61	-7.9
	luteolin	5280445	-113.43	-8.0
	apigenin	5280443	-99.62	-7.9
	isoramnetin	5280681	-115.09	-7.8
	pedalitin	31161	-106.91	-8.4
	scutellarein	5281697	-103.01	-8.1

Table 2 (*continue*). Binding energies and affinities of 88 ligands selected from *Verbena officinalis* to the G6PDH protein structure

Group of metabolites	Compounds	Pubchem CID	Binding energy (kcal/mol)	Binding affinity (kcal/mol)
Phenolic acids				
	ferulic acid	445858	-89.4	-5.7
	protocatechuic acid	72	-79.14	-6.1
Terpenoids				
Diterpenoids				
	carnosol	442009	-87	-7.3
	carnosolic acid	11566445	-95.84	-6.8
	rosmanol	13966122	-107.9	-7.4
	isorosmanol	13820511		
triterpenoids				
	ursolic acid	64945	-93.05	-7.3
	3-epiursolic acid	7163177	-92.56	-7.4
Carbohydrates				
	arabinose	439195	-76.72	-4.8
	galactose	6036	-88.74	-5.1
	galacturonic acid	439215	-88.81	-5.9
	glucose	5793	-89.43	-5.1
	mannose	18950	-89.38	-5.1
	rhamnose	25310	-89.39	-5.1
	xylose	135191	-76.76	-4.8
Sterols				
	stigmasterol	5280794	-84.63	-7.5
	β-sitosterol	222284	-87	-7.2
Fatty acids				
	cornudentanone	442735	-107.57	'-6.4
	oleic acid	445639	-97.4	-5.8
	3-epioleanolic acid	11869658	-84.79	-7.0
Essential oil				
Monoterpenoids				
	isobornyl formate	23623868	-63.99	-5.2
	citral (geranial)	638011	-69.47	-5.6
	limonene	22311	-59.84	-5.7
	carvone	7439	-71.11	-6.1
	1.8-cineole	2758	-44.6	-5.0
	hepten-3-one	520420	-59.21	-4.5
	α-terpineol	17100	-67.04	-5.7
	anethole	637563	-72.34	-5.6
	β-pinene	14896	-45.68	-4.7
	thymol	6989	-69.74	-5.8
	methyl heptenone	9862	-61.29	-5.1

Table 2 (*continue*). Binding energies and affinities of 88 ligands selected from *Verbena officinalis* to the G6PDH protein structure

Group of metabolites	Compounds	Pubchem CID	Binding energy (kcal/mol)	Binding affinity (kcal/mol)
	carvacrol	10364	-70.69	-6.3
	trans-carveol	94221	-64.7	-5.2
	isopiperitone	6987	-67.86	-5.9
	α-pinene	82227	-46.83	-4.7
	piperitone	6987	-67.86	-5.9
	cis-carveol	330573	-64.72	-5.2
	terpinen-4-ol	11230	-66.84	-5.4
	β-phellandrene	11142	-57.18	-5.8
	geraniol	637566	-63.19	-5.7
	β-terpineol	8748	-68.77	-5.5
	sabinene	18818	-51.84	-5.0
	cinerone	5373127	-70.66	-6.3
	p-cymene	7463	-59.45	-6.1
	nerol	643820	-67.54	-5.6
	linalol	6549	-63.08	-5.1
	(E)-β-ocimene	5281553	-56.55	-5.4
	borneol	64685	-47.57	-4.8
	iso-pinocamphone	84532	-53.62	-5.1
	o-cymene	10703	-57.57	-6.2
	γ-terpinene	7461	-58.9	-5.9
Sesquiterpenoids				
	caryophyllene oxide	1742210	-65.75	-5.8
	spathulenol	92231	-65.47	-5.8
	α-curcumane	92139	-74.51	-6.7
	β-caryophyllene	5281515	-58.27	-5.5
	trans-nerolidol	5284507	-71.01	-6.2
	bicyclosesquiphellandrene	521496	-69.8	-6.4
	δ-cadinene	441005	-64.75	-6.2
	β-bourbonene	62566	-62.14	-6.1
	allo-aromadendrene	42608158	-58.6	-5.7
	α-cubenene	442359	-68.22	-6.1
	γ-cadinene	6432404	-67.12	-6.4
	germacene D	5317570	-71.04	-6.1
	α-muurolene	12306047	-69.57	-6.4
	bicyclogermacrene	13894537	-60.4	-5.3
	cis-muurola-4(14).5-diene	51351709	-71.4	-6.4
	isocaryophylene oxide	1742211	-65.87	-5.8
	β-cedrene	11106485	-56.85	-6.1
	α-copaene	92042749	-58.92	-5.7
	β-elemene	6918391	-64.58	-5.9

Table 2 (*continue*). Binding energies and affinities of 88 ligands selected from *Verbena officinalis* to the G6PDH protein structure

Group of metabolites	Compounds	Pubchem CID	Binding energy (kcal/mol)	Binding affinity (kcal/mol)
	β-cubenene	93081	-63.08	-6.2
	α-humulene	5281520	-65.95	-5.7
	α-7-epi-selinene	91753195	-64.13	-6.0
	isoledene	530426	-60.38	-5.9

This list indicates the chemicals that comply with Lipinski's Rule of 5

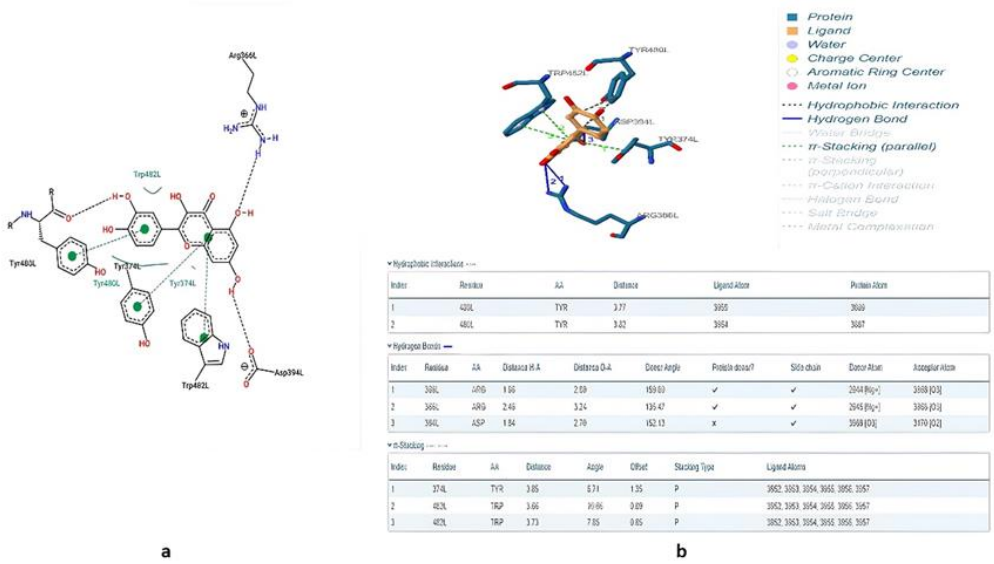

Figure 1. The 2D (a) and 3D (b) interaction poses of quercetin and G6PD complex

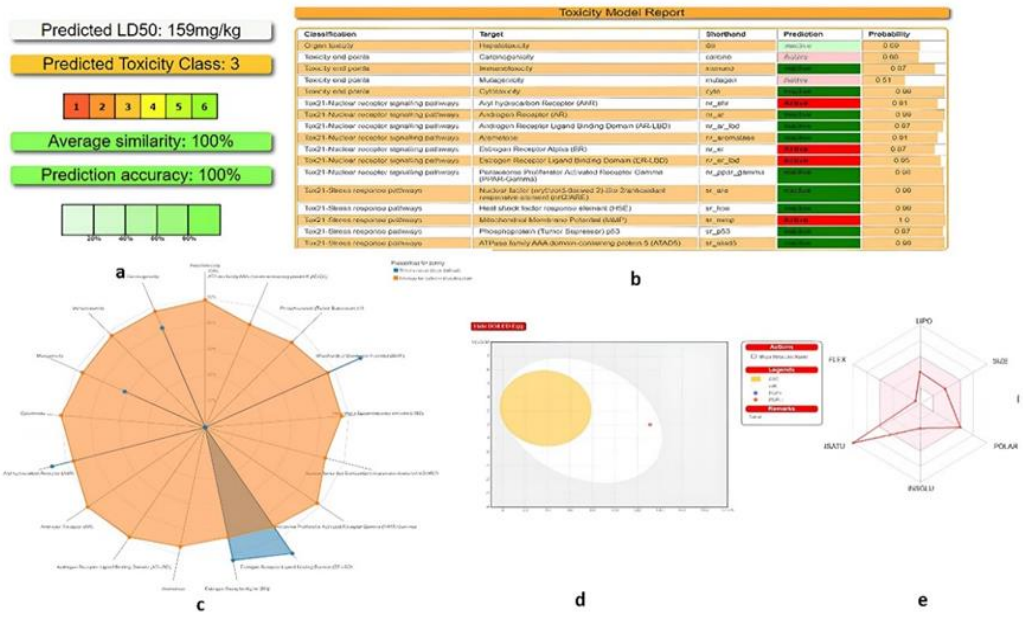

Figure 2. Toxicity results of quercetin calculated with Pro ToX-II (a, b), BOILED Egg model calculated with Swiss ADME (d) and radar graph for physicochemical properties of quercetin (e)

The Root Mean Square Deviation (RMSD), determines how much the atomic positions in a simulation deviate from a reference structure, typically the starting point [48]. During equilibration, the

RMSD typically increases as the system adjusts from its initial state. Once the simulation reaches equilibrium, the RMSD should fluctuate around a stable value, indicating the atoms are sampling their allowed conformations. This stable RMSD signifies the system is ready for the data collection phase of the MD simulation. The root mean square deviation plot of the overall simulation at 310 K is given in Figure 3. It can be seen from these plots that our system was equilibrated after 5.6 ns. Therefore, the first 5.6-nanosecond-long simulation is considered as equilibration period and excluded from further investigation. Moreover, the RMSD plot suggests minimal conformational change during the production period. The Root Mean Square Fluctuation (RMSF) values (Figure 4) per residue has shown that the solvent-exposed residues such as Ile353, Met384 and Asn403 contribute the most to the molecular motion throughout the simulation. After concluding the 300-ns-long MD simulation, a clustering analysis based on a "hierarchical agglomerative" approach was performed for post-processing of the trajectories. The cluster radii are set to 2.0, this cluster analysis in the G6PD-quercetin complex had produced three conformations and the percentage of the occurrences of each cluster were 84%, 10% and 6%. The most populated cluster, containing 84% of the data points, suggests that the G6PD-quercetin complex primarily adopts a single conformation during the simulation. The most populated cluster is shown in Figure 5. During the MD simulation, the quercetin molecule stays in the active site and interacts with several residues. For instance, the quercetin makes pi-stacking interactions with the Tyr374. Also, Asp394 is coordinated with one of the -OH group of quercetin, and backbone oxygen atom of Lys481 makes a hydrogen bond with another -OH group of quercetin. These interactions can be seen clearly in the most-populated cluster, which is shown in detail in Figure 6. The results have shown that the position of this quercetin molecule is very well defined, and the molecule is stable in this region. To prove their importance, these acidic and basic residues could be mutated to nonpolar amino acids, and further MD simulations could be done to check the activities in this state.

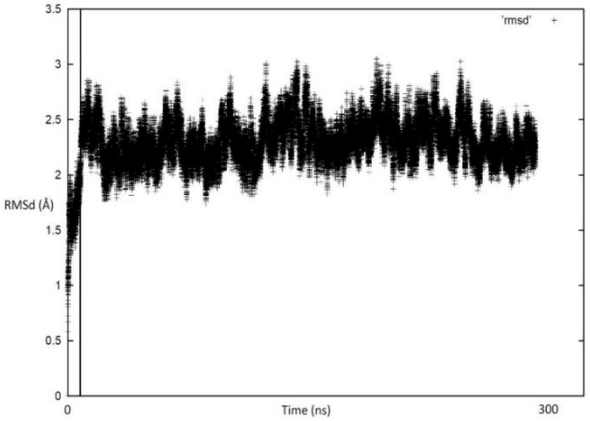

Figure 3. RMSD graph of the simulation. The left-side of the dash represents the equilibration time

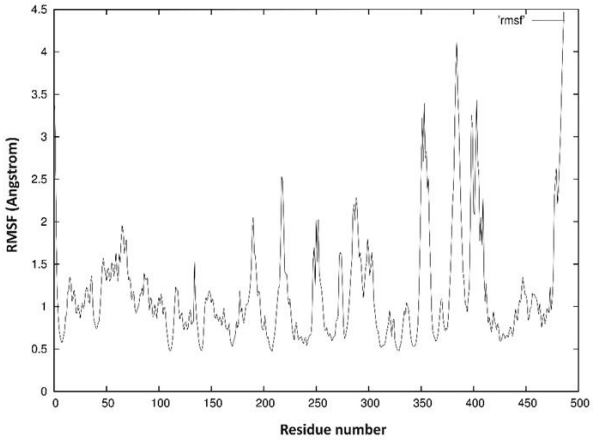

Figure 4. RMSF values at 310 K

Figure 5. The most-populated cluster of the G6PD-quercetin complex

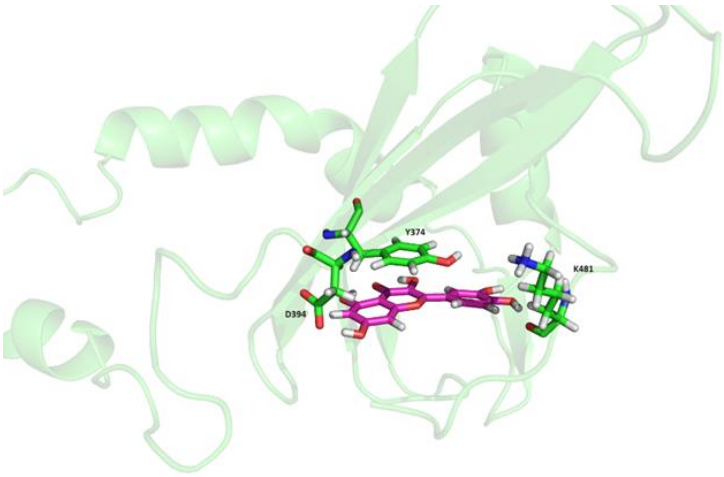

Figure 6. Close contacts between quercetin and its nearby residues in the most-populated cluster

ADME results have shown that quercetin complies with the limits set by the Lipinski rule and supports oral use and drug similarity. In the radar chart taken in SwissADME, the distribution of important physicochemical properties in our body has been created (Table 1, Figure 2d and e). In the pictures of BOILED Eggs, the white and yellow area respectively indicate passive absorption in the gastrointestinal (GI) tract and the ability to cross the blood-brain barrier (BBB). The outer grey area indicates molecules with low absorption and limited brain penetration (Figure 2d) [49]. According to the ADME profile, it has been stated that quercetin does not cross the blood brain barrier.

When the pink range was analysed (Figure 2e), lipophilicity (LIPO; iLOGP), size (MW), polarity (TPSA), solubility (INSOLU, log S), saturation (INSATU; carbon fraction in sp^3 hybridization was found to be 0) and flexibility (FLEX, rotatable bonds) are in the optimal range for quercetin. Deviation in saturation was observed. Molecules that are more saturated and have sp^3 hybridization are generally more water soluble and may be biologically effective. Nevertheless, a thorough examination of pharmacodynamics requires an all-encompassing viewpoint. The analysis results proved that the five properties were in the pink area and the compound fit into the group of drug-like compounds. Based on these properties, it can be said that the compound is not suitable for injectable administration due to its low flexibility [50].

In the BOILED Egg model, blue and red dots indicate P-glycoprotein (P-gp) substrates (PGP+), which is an ATP-dependent transmembrane protein that transports many drugs, and non-P-gp substrates (PGP−), respectively. While it is an advantage for a drug that is not a P-gp substrate to remain in the target cell for a longer time and interact less with other drugs, it is a disadvantage because the drug's tendency to remain in the body for a longer time will lead to toxicity [51]. Based on this, if the drug's

elimination from the body is to be accelerated, it may need to be designed as a P-gp substrate. Whether or not a compound is a P-gp substrate affects the efficacy and pharmacokinetics of the drug. These considerations need to be acknowledged throughout the drug development process.

Computational studies on absorption, distribution, metabolism, and excretion have reported that the ability of quercetin to combine with the plasma-protective protein varies between 85.36% and 99.82%. These studies also examined quercetin and their ADME properties, revealing that quercetin and 3′-methyl ether quercetin had 100% passive absorption, while other quercetin cells showed a lower absorption [41]. The fact that ADME, which has a very satisfactory predictive power in molecular design, states that quercetin does not cross the blood brain barrier may be due to the limited prediction of penetration of BOILED Egg [49,53]. The *in silico* interaction of geroprotective phytochemicals, including quercetin, with Sirtuin 1 was examined, and ADME results showed that quercetin could not cross the BBB and was toxic (class 3). However, animal studies have reported that quercetin can be tolerated at oral doses above the LD_{50} value [54] and is a safe nutritional supplement in mice [55]. For this reason, pharmacological toxicology studies on quercetin should be conducted.

In the Protox II analysis, the lethal dose 50 (LD_{50}) value of quercetin was estimated as 159 mg/kg and toxicity class 3. The toxicity model report of our study shows that quercetin is a carcinogenic and mutagenic structure, also has various interfering effects against Aryl Hydrocarbon Receptor (AhR), Estrogen Receptor Alpha (ER), Estrogen Receptor Ligand Binding Domain (ER-LBD) and Mitochondrial Membrane Potential (MMP) (Figure 2a-c).

It is extremely important to perform *in silico* toxicity analyses, examine drug candidates and perform risk assessments before clinical studies [56,57]. The fact that an antioxidant structure also has carcinogenic and mutagenic properties according to *in silico* toxicity analysis results may indicate that the compound may affect different cellular or molecular targets [58]. The effects of compounds are related to dose and prolonged exposure times. While a particular compound may have antioxidant effects at low doses, it may cause toxic effects at high doses [59]. The compounds are metabolized and biotransformed in the body. These processes can greatly affect the effects of the compound. For example, when quercetin is metabolized in the body, different products can be formed, some of which may be more toxic. The compound's targets and mechanisms of action can regulate a variety of biological responses. Binding of quercetin to targets such as AhR [60], ER [61], ER-LBD [62] and MMP [63] can affect different biological processes [64]. A study in 2010 emphasized the vulnerability of individuals with G6PD deficiency to oxidative stress and assessed the protective effects of the flavonoid quercetin against oxidative damage induced by H_2O_2. The research demonstrated that quercetin not only exhibits antioxidant properties but also offers cellular protection [43]. The investigations' findings in 2016, supported by numerous experiments, shed light on the mechanisms by which quercetin may protect against neurotoxicity, neuronal injury, and neurodegenerative diseases, offering potential therapeutic avenues for neurological disorders [65]. In a different 2018 research, quercetin's potential as an effective anticancer agent was highlighted. The study proposed that quercetin could influence O-GlcNAcylation, a process associated with cancer, warranting further investigation into its specific mechanisms for cancer treatment [66].

Moreover, recent findings have underscored the significant role of quercetin in combating liver cancer. Quercetin is shown to regulate intracellular processes, inhibiting the cell cycle and promoting apoptosis, which leads to the death of cancer cells. Consequently, this naturally occurring compound, found in plants, is being considered as a promising candidate for the development of novel anticancer drugs [58]. Molecular level analyses and predictions applied used the drug development process were applied to the phytochemical drug candidates in *V. officinalis*. Quercetin, the structure that computer-based analyses lead us to, has been shown to be effective in fighting liver cancer in *in vivo* experiments.

Within the scope of the study, in order to evaluate the potential of the new complex and direct it to clinical research; In addition to *in vitro* studies examining its effects on liver cancer cell lines in more detail, experiments can be conducted to evaluate the effects of the complex *in vivo* models. Optimization of the structure should also be provided to increase the effectiveness and safety of the drug.

AUTHOR CONTRIBUTIONS

Concept: H.A.; Design: H.A.; Control: H.A.; Sources: H.A.; Materials: H.A.; Data Collection and/or Processing: H.A.; Analysis and/or Interpretation: H.A., A.Ö; Literature Review: H.A.; Manuscript Writing: H.A., A.Ö.; Critical Review: H.A., A.Ö.; Other: -

CONFLICT OF INTEREST

The authors declare that there is no real, potential, or perceived conflict of interest for this article.

ETHICS COMMITTEE APPROVAL

The authors declare that the ethics committee approval is not required for this study.

REFERENCES

1. Prieto-Martínez, F.D., López-López, E., Eurídice Juárez-Mercado, K., MedinaFranco, J.L. (2019). Computational drug design methods-current and future perspectives, in *in silico* drug design. Academic Press, p. 19-44. [CrossRef]
2. López-López, E., Bajorath, J., Medina-Franco, J.L. (2021). Informatics for chemistry, biology, and biomedical sciences. Journal of Chemical Infori Modeling, 61 (1), 26-35. [CrossRef]
3. Medina-Franco, J.L., Martinez-Mayorga, K., Fernández-de Gortari, E., Kirchmair, J., Bajorath, J. (2021). Rationality over fashion and hype in drug design. F1000Research, 10, Chem Inf Sci-397. [CrossRef]
4. Stuart, J. (2014). Herbal medicines. Fourth edition. Journal of the Medical Library Association: Journal of the Medical Library Association, 102(3), 222-223. [CrossRef]
5. Ghazanfar, S.A. (1994). Handbook of Arabian Medicinal Plants, CRC Press, Boca Raton, Florida, p. 176. [CrossRef]
6. Kubica, P., Szopa, A., Dominiak, J., Luczkiewicz, M., Ekiert, H. (2020). *Verbena officinalis* (Common Vervain)-A Review on the investigations of this medicinally important plant species. Planta Medica, 86(17). [CrossRef]
7. Rehecho, S., Hidalgo, O., de Cirano, M. G.I., Navarro, I., Astiasarán, I., Ansorena, D., Cavero, R.Y., Calvo, M.I. (2011). Chemical composition, mineral content and antioxidant activity of *Verbena officinalis* L. LWT-Food Science and Technology, 44 (4), 875-882. [CrossRef]
8. Liu, Z., Xu, Z., Zhou, H., Cao, G., Cong, X.D., Zhang, Y., Cai, B.C. (2012). Simultaneous determination of four bioactive compounds in *Verbena officinalis* L. by using high-performance liquid chromatography. Pharmacognosy Magazine, 8(30), 162-165. [CrossRef]
9. Van Wyk, B.E., Wink, M. (2017). Medicinal Plants of The World, Cabi, London, p.520.
10. Akour, A., Kasabri, V., Afifi, F.U., Bulatova, N. (2016). The use of medicinal herbs in gynecological and pregnancy-related disorders by Jordanian women: A review of folkloric practice vs. evidence-based pharmacology. Pharmaceutical Biology, 54(9), 1901-1918. [CrossRef]
11. Khan, A.W., Khan, A.U., Ahmed, T. (2016). Anticonvulsant, anxiolytic, and sedative activities of *Verbena officinalis*. Frontiers in Pharmacology, 7, 499. [CrossRef]
12. Lai, S.W., Yu, M.S., Yuen, W.H., Chang, R.C. (2006). Novel neuroprotective effects of the aqueous extracts from *Verbena officinalis* Linn. Neuropharmacology, 50(6), 641-650. [CrossRef]
13. Ashok Kumar, B.S., Lakshman, K., Velmurugan, C., Sridhar, S.M., Gopisetty, S. (2014). Antidepressant activity of methanolic extract of amaranthus spinosus. Basic and Clinical Neuroscience, 5(1), 11-17.
14. De Martino, L., D'Arena, G., Minervini, M.M., Deaglio, S., Fusco, B.M., Cascavilla, N., De Feo, V. (2009). *Verbena officinalis* essential oil and its component citral as apoptotic-inducing agent in chronic lymphocytic leukemia. International Journal of Immunopathology and Pharmacology, 22(4), 1097-1104. [CrossRef]
15. Speroni, E., Cervellati, R., Costa, S., Guerra, M.C., Utan, A., Govoni, P., Berger, A., Müller, A., Stuppner, H. (2007). Effects of differential extraction of *Verbena officinalis* on rat models of inflammation, cicatrization and gastric damage. Planta Medica, 73(3), 227-235. [CrossRef]
16. Calvo M.I. (2006). Anti-inflammatory and analgesic activity of the topical preparation of *Verbena officinalis* L. Journal of Ethnopharmacology, 107(3), 380-382. [CrossRef]
17. Casanova, E., García-Mina, J.M., Calvo, M.I. (2008). Antioxidant and antifungal activity of *Verbena officinalis* L. leaves. Plant Foods for Human Nutrition (Dordrecht, Netherlands), 63(3), 93-97. [CrossRef]
18. Li, Y. (2008). Chinese medicinal herbs for effectively treating cirrhosis, in liver ascites. CN101244158.

19. Zhang, S., Gu, H., Zhang, W., Li, X., Li, Y., Liu, B., Wang, M., Zhang, X. (2008). Chinese medicine composition for treating nephropathy. CN101313971i.
20. Hu, S. (2008). Chinese medicine for treating prostatitis and hyperplasia. CN101195011.
21. Yang, H.C., Wu, Y.H., Liu, H.Y., Stern, A., Chiu, D.T. (2016). What has passed is prolog: New cellular and physiological roles of G6PD. Free Radical Research, 50(10), 1047-1064. [CrossRef]
22. Patra, K.C., Hay, N. (2014). The pentose phosphate pathway and cancer. Trends in Biochemical Sciences, 39(8), 347-354. [CrossRef]
23. Liu, B., Fu, X., Du, Y., Feng, Z., Chen, R., Liu, X., Yu, F., Zhou, G., Ba, Y. (2023). Pan-cancer analysis of G6PD carcinogenesis in human tumors. Carcinogenesis, 44(6), 525-534. [CrossRef]
24. Yang, H.C., Stern, A., Chiu, D.T. (2021). G6PD: A hub for metabolic reprogramming and redox signaling in cancer. Biomedical Journal, 44(3), 285-292. [CrossRef]
25. Li, R., Ke, M., Qi, M., Han, Z., Cao, Y., Deng, Z., Qian, J., Yang, Y., Gu, C. (2022). G6PD promotes cell proliferation and dexamethasone resistance in multiple myeloma via increasing anti-oxidant production and activating Wnt/β-catenin pathway. Experimental Hematology & Oncology, 11(1), 77. [CrossRef]
26. Sun, L., Suo, C., Li, S.T., Zhang, H., Gao, P. (2018). Metabolic reprogramming for cancer cells and their microenvironment: Beyond the Warburg Effect. Biochimica et Biophysica Acta-Reviews on Cancer, 1870(1), 51-66. [CrossRef]
27. Li, R., Wang, W., Yang, Y., Gu, C. (2020). Exploring the role of glucose-6-phosphate dehydrogenase in cancer (Review). Oncology Reports, 44(6), 2325-2336. [CrossRef]
28. Butt, S.S., Badshah, Y., Shabbir, M., Rafiq, M. (2020). Molecular docking using chimera and autodock vina software for nonbioinformaticians. JMIR Bioinformatics and Biotechnology, 1(1), e14232. [CrossRef]
29. Setlur, A.S., Chandrashekar, K., Panhalkar, V., Sharma, S., Sarkar, M., Niranjan, V. (2023). *In-silico*-based toxicity investigation of natural repellent molecules against the human proteome: A safety profile design. Protocols.io, 83767. [CrossRef]
30. Chen, Y., Gan, Y., Yu, J., Ye, X., Yu, W. (2023). Key ingredients in *Verbena officinalis* and determination of their anti-atherosclerotic effect using a computer-aided drug design approach. Frontiers in Plant Science, 14, 1154266. [CrossRef]
31. Goddard, T.D., Huang, C.C, Ferrin, T.E. (2007). Visualizing density maps with UCSF Chimera. Journal of Structural Biology, 157(1), 281-287. [CrossRef]
32. Del Águila Conde, M., Febbraio, F. (2022). Risk assessment of honey bee stressors based on *in silico* analysis of molecular interactions. EFSA Journal- European Food Safety Authority, 20(Suppl 2), e200912. [CrossRef]
33. Chen, X., Li, H., Tian, L., Li, Q., Luo, J., Zhang, Y. (2020). Analysis of the physicochemical properties of acaricides based on Lipinski's Rule of five. Journal of Computational Biology: A Journal of Computational Molecular Cell Biology, 27(9), 1397-1406. [CrossRef]
34. Kalay, Ş., Akkaya, H. (2023). Molecular modelling of some ligands against acetylcholinesterase to treat Alzheimer's Disease. Journal of Research Pharmacy, 27(6), 2199-2209. [CrossRef]
35. Maier, J.A., Martinez, C., Kasavajhala, K., Wickstrom, L., Hauser, K.E., Simmerling, C. (2015). ff14SB: Improving the accuracy of protein side chain and backbone parameters from ff99SB. Journal of Chemical Theory and Computation, 11(8), 3696-3713. [CrossRef]
36. Jorgensen, W.L., Chandrasekhar, J., Madura, J.D. (1983). Comparison of simple potential functions for simulating liquid water. The Journal of Chemical Physics, 79, 926-935. [CrossRef]
37. Adasme, M.F., Linnemann, K.L., Bolz, S.N., Kaiser, F., Salentin, S., Haupt, V.J., Schroeder, M. (2021). PLIP 2021: Expanding the scope of the protein-ligand interaction profiler to DNA and RNA. Nucleic Acids Research, 49(W1), 530-534. [CrossRef]
38. Case, D.A., Betz, R.M., Cerutti, D.S., Cheatham, III, T.E., Darden, T.A., Duke, R.E., Giese, T.J., Gohlke, H., Goetz, A.W., Homeyer, N., Izadi, S., Janowski, P., Kaus, J., Kovalenko, A., Lee, T.S., LeGrand, S., Li, P., Lin, C., Luchko, T., Luo, R., Madej, B., Mermelstein, D., Merz, K.M., Monard, G., Nguyen, H., Nguyen, H.T., Omelyan, I., Onufriev, A., Roe, D.R., Roitberg, A., Sagui, C., Simmerling, C.L., Botello-Smith, W.M., Swails, J., Walker, R.C., Wang, J., Wolf, R.M., Wu, X., Xiao, L., Kollman, P.A. (2016). AMBER 2016, University of California, San Francisco.
39. Sumera, Anwer, F., Waseem, M., Fatima, A., Malik, N., Ali, A., Zahid, S. (2022). Molecular docking and molecular dynamics studies reveal secretory proteins as novel targets of temozolomide in glioblastoma multiforme. Molecules, 27(21), 7198. [CrossRef]
40. Ghosh, P., Bhakta, S., Bhattacharya, M., Sharma, A.R., Sharma, G., Lee, S.S., Chakraborty, C. (2021). A novel multi-epitopic peptide vaccine candidate against *Helicobacter pylori*: *In-Silico* identification, design, cloning and validation through molecular dynamics. International Journal of Peptide Research and Therapeutics, 27(2), 1149-1166. [CrossRef]

41. Shah, S.A.A., Qureshi, N.A., Qureshi, M.Z., Alhewairini, S.S., Saleem, A., Zeb, A. (2023). Characterization and bioactivities of *M. arvensis*, *V. officinalis* and *P. glabrum*: *In-silico* modeling of *V. officinalis* as a potential drug source. Saudi Journal of Biological Sciences, 30(6), 103646. [CrossRef]
42. Nisar, R., Ahmad, S., Khan, K.U., Sherif, A.E., Alasmari, F., Almuqati, A.F., Ovatlarnporn, C., Khan, M. A., Umair, M., Rao, H., Ghalloo, B.A., Khurshid, U., Dilshad, R., Nassar, K.S., Korma, S.A. (2022). Metabolic Profiling by GC-MS, *in vitro* biological potential, and *ın silico* molecular docking studies of *Verbena officinalis*. Molecules, 27(19), 6685. [CrossRef]
43. Jamshidzadeh, A., Rezaeian Mehrabadi, A. (2010). Protective effect of quercetin on oxidative stress in glucose-6-phosphate dehydrogenase-deficient erythrocytes *in vitro*. Iranian Journal of Pharmaceutical Research: IJPR, 9(2), 169-175. [CrossRef]
44. Anandan, S., Gowtham, H.G., Shivakumara, C.S., Thampy, A., Singh, S.B., Murali, M., Shivamallu, C., Pradeep, S., Shilpa, N., Shati, A.A., Alfaifi, M.Y., Elbehairi, S.E.I., Ortega-Castro, J., Frau, J., Flores-Holguín, N., Kollur, S.P., Glossman-Mitnik, D. (2022). Integrated approach for studying bioactive compounds from *Cladosporium* spp. against estrogen receptor alpha as breast cancer drug target. Scientific Reports, 12(1), 22446. [CrossRef]
45. Bissantz, C., Kuhn, B., Stahl, M. (2010). A medicinal chemist's guide to molecular interactions. Journal of Medicinal Chemistry, 53(14), 5061-5084. [CrossRef]
46. Hwang, S., Mruk, K., Rahighi, S., Raub, A.G., Chen, C.H., Dorn, L.E., Horikoshi, N., Wakatsuki, S., Chen, J.K., Mochly-Rosen, D. (2018). Correcting glucose-6-phosphate dehydrogenase deficiency with a small-molecule activator. Nature Communications, 9(1), 4045. [CrossRef]
47. Ge, Z., Xu, M., Ge, Y., Huang, G., Chen, D., Ye, X., Xiao, Y., Zhu, H., Yin, R., Shen, H., Ma, G., Qi, L., Wei, G., Li, D., Wei, S., Zhu, M., Ma, H., Shi, Z., Wang, X., Ge, X., Qian, X. (2023). Inhibiting G6PD by quercetin promotes degradation of EGFR T790M mutation. Cell Reports, 42(11), 113417. [CrossRef]
48. Knapp, B., Frantal, S., Cibena, M., Schreiner, W., Bauer, P. (2011). Is an intuitive convergence definition of molecular dynamics simulations solely based on the root mean square deviation possible? Journal of Computational Biology, 18(8), 997-1005. [CrossRef]
49. Montanari, F., Ecker, G.F. (2015). Prediction of drug-ABC-transporter interaction-recent advances and future challenges. Advanced Drug Delivery Reviews, 86, 17-26. [CrossRef]
50. Poczta, A., Krzeczyński, P., Tobiasz, J., Rogalska, A., Gajek, A., Marczak, A. (2022). Synthesis and *in vitro* activity of novel melphalan analogs in hematological malignancy cells. International Journal of Molecular Sciences, 23(3), 1760. [CrossRef]
51. Hennessy, M., Spiers, J.P. (2007). A primer on the mechanics of P-glycoprotein the multidrug transporter. Pharmacological Research, 55(1), 1-15. [CrossRef]
52. Simanjuntak, K., Simanjuntak, J.E., Prasasty, V.D. (2017). Structure-based drug design of quercetin and its derivatives against HMGB1. Biomedical and Pharmacology Journal. 10 (4), 1973-1982. [CrossRef]
53. Daina, A., Michielin, O., Zoete, V. (2017). SwissADME: A free web tool to evaluate pharmacokinetics, drug-likeness and medicinal chemistry friendliness of small molecules. Scientific Reports, 7, 42717. [CrossRef]
54. Medoro, A., Jafar, T.H., Ali, S., Trung, T.T., Sorrenti, V., Intrieri, M., Scapagnini, G., Davinelli, S. (2023). *In silico* evaluation of geroprotective phytochemicals as potential sirtuin 1 interactors. Biomedicine & Pharmacotherapy = Biomedecine & Pharmacotherapie, 161, 114425. [CrossRef]
55. David, S., Cunningham, R. (2019). Echinacea for the prevention and treatment of upper respiratory tract infections: A systematic review and meta-analysis. Complementary Therapies in Medicine, 44, 18-26. [CrossRef]
56. Saini, N., Bakshi, S., Sharma, S. (2018). *In-silico* approach for drug induced liver injury prediction: Recent advances. Toxicology Letters, 295, 288-295. [CrossRef]
57. Kelleci Çelik, F., Karaduman, G. (2023). Machine learning-based prediction of drug-induced hepatotoxicity: An OvA-QSTR approach. Journal of Chemical Information and Modeling, 63(15), 4602-4614. [CrossRef]
58. Sethi, G., Rath, P., Chauhan, A., Ranjan, A., Choudhary, R., Ramniwas, S., Sak, K., Aggarwal, D., Rani, I., Tuli, H.S. (2023). Apoptotic mechanisms of quercetin in liver cancer: Recent trends and advancements. Pharmaceutics, 15(2), 712. [CrossRef]
59. Bouayed, J., Bohn, T. (2010). Exogenous antioxidants-double-edged swords in cellular redox state: Health beneficial effects at physiologic doses versus deleterious effects at high doses. Oxidative Medicine and Cellular Longevity, 3(4), 228-237. [CrossRef]
60. Vrba, J., Kren, V., Vacek, J., Papouskova, B., Ulrichova, J. (2012). Quercetin, quercetin glycosides and taxifolin differ in their ability to induce AhR activation and CYP1A1 expression in HepG2 cells. Phytotherapy Research: PTR, 26(11), 1746-1752. [CrossRef]

61. Wang, Z., Zhang, G., Le, Y., Ju, J., Zhang, P., Wan, D., Zhao, Q., Jin, G., Su, H., Liu, J., Feng, J., Fu, Y., Hou, R. (2020). Quercetin promotes human epidermal stem cell proliferation through the estrogen receptor/β-catenin/c-Myc/cyclin A2 signaling pathway. Acta Biochimica et Biophysica Sinica, 52(10), 1102-1110. [CrossRef]
62. Caltagirone, S., Ranelletti, F.O., Rinelli, A., Maggiano, N., Colasante, A., Musiani, P., Aiello, F.B., Piantelli, M. (1997). Interaction with type II estrogen binding sites and antiproliferative activity of tamoxifen and quercetin in human non-small-cell lung cancer. American Journal of Respiratory Cell and Molecular Biology, 17(1), 51-59. [CrossRef]
63. Vijayababu, M.R., Arunkumar, A., Kanagaraj, P., Venkataraman, P., Krishnamoorthy, G., Arunakaran, J. (2006). Quercetin downregulates matrix metalloproteinases 2 and 9 proteins expression in prostate cancer cells (PC-3). Molecular and Cellular Biochemistry, 287(1-2), 109-116. [CrossRef]
64. Mirazimi, S.M.A., Dashti, F., Tobeiha, M., Shahini, A., Jafari, R., Khoddami, M., Sheida, A.H., EsnaAshari, P., Aflatoonian, A.H., Elikaii, F., Zakeri, M.S., Hamblin, M.R., Aghajani, M., Bavarsadkarimi, M., Mirzaei, H. (2022). Application of quercetin in the treatment of gastrointestinal cancers. Frontiers in Pharmacology, 13, 860209. [CrossRef]
65. Costa, L.G., Garrick, J.M., Roquè, P.J., Pellacani, C. (2016). Mechanisms of neuroprotection by quercetin: Counteracting oxidative stress and more. Oxidative Medicine and Cellular Longevity, 2016, 2986796. [CrossRef]
66. Ali, A., Kim, M.J., Kim, M.Y., Lee, H.J., Roh, G.S., Kim, H.J., Cho, G.J., Choi, W.S. (2018). Quercetin induces cell death in cervical cancer by reducing O-GlcNAcylation of adenosine monophosphate-activated protein kinase. Anatomy & Cell Biology, 51(4), 274-283. [CrossRef]